Spectrochimica Acta Part A: Molecular and Biomolecular Spectroscopy 265 (2022) 120381

Contents lists available at ScienceDirect

Spectrochimica Acta Part A: Molecular and Biomolecular Spectroscopy

journal homepage: www.elsevier.com/locate/saa

Laser induced degradation of bacterial spores during micro-Raman spectroscopy

Dmitry Malyshev [a], Rasmus Öberg [a], Tobias Dahlberg [a], Krister Wiklund [a], Lars Landström [b], Per Ola Andersson [b,c], Magnus Andersson [a,d,*]

[a] Dept of Physics, Umeå University, 901 87 Umeå, Sweden
[b] Swedish Defence Research Agency (FOI), Umeå, Sweden
[c] Department of Engineering Sciences, Uppsala University, Uppsala, Sweden
[d] Umeå Centre for Microbial Research (UCMR), Umeå, Sweden

HIGHLIGHTS

- NIR laser light in optical tweezers can disrupt the body of thermal-resistant bacterial spores.
- A dose exposure of 60 Joules causes notable alterations of the structure of a spore.
- Spore damage is related to a photochemical effect rather than photothermal.

GRAPHICAL ABSTRACT

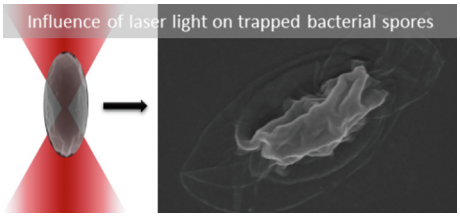

ARTICLE INFO

Article history:
Received 26 March 2021
Received in revised form 9 August 2021
Accepted 6 September 2021
Available online 12 September 2021

Keywords:
Raman spectroscopy
Spores
Decontamination
Optical tweezers
Multiphysics modelling
Bacteria

ABSTRACT

Micro-Raman spectroscopy combined with optical tweezers is a powerful method to analyze how the biochemical composition and molecular structures of individual biological objects change with time. In this work we investigate laser induced effects in the trapped object. *Bacillus thuringiensis* spores, which are robust organisms known for their resilience to light, heat, and chemicals are used for this study. We trap spores and monitor the Raman peak from CaDPA (calcium dipicolinic acid), which is a chemical protecting the spore core. We see a correlation between the amount of laser power used in the trap and the release of CaDPA from the spore. At a laser power of 5 mW, the CaDPA from spores in water suspension remain intact over the 90 min experiment, however, at higher laser powers an induced effect could be observed. SEM images of laser exposed spores (after loss of CaDPA Raman peak was confirmed) show a notable alteration of the spores' structure. Our Raman data indicates that the median dose exposure to lose the CaDPA peak was ~60 J at 808 nm. For decontaminated/deactivated spores, i.e., treated in sodium hypochlorite or peracetic acid solutions, the sensitivity on laser power is even more pronounced and different behavior could be observed on spores treated by the two chemicals. Importantly, the observed effect is most likely photochemical since the increase of the spore temperature is in the order of 0.1 K as suggested by our numerical multiphysics model. Our results show that care must be taken when using micro-Raman spectroscopy on biological objects since photoinduced effects may substantially affect the results.

© 2021 The Author(s). Published by Elsevier B.V. This is an open access article under the CC BY license (http://creativecommons.org/licenses/by/4.0/).

1. Introduction

Laser Tweezers Raman spectroscopy (LTRS) is a powerful analytical and reagentless method that provides a biochemical fingerprint of a trapped biological object. For example, LTRS can trap and

* Corresponding author at: Dept of Physics, Umeå University, 901 87 Umeå, Sweden.
E-mail address: magnus.andersson@umu.se (M. Andersson).

https://doi.org/10.1016/j.saa.2021.120381
1386-1425/© 2021 The Author(s). Published by Elsevier B.V.
This is an open access article under the CC BY license (http://creativecommons.org/licenses/by/4.0/).

simultaneously analyze eukaryotic cells, bacteria, and spores [1]. In general, trapping different objects has been considered non-invasive at low laser power [2]. However, even though the laser power used may be low, the strongly focused beam results in a high-intensity spot ~MW/cm^2, possibly capable of causing photo-damage to the trapped object. Previous studies have assessed how optical traps cause damage to living cells, where early investigations indicated no DNA damage to cells with laser powers up to 100 mW in eukaryotic cells [3]. In contrast, later studies noted a decrease in viability of cells trapped using optical tweezers and a dose-related relationship between total irradiance and cell viability could be observed. The proposed mechanisms of action were absorbance of light by NADH and flavins for laser light in the 650–750 nm range, and absorbance by water at wavelengths 800–1064 nm [4,5], leading to DNA damage [5]. In these studies, wavelengths in the region 800 nm and 1064 nm were found to be the least damaging to the cells. However, reactive oxygen species (ROS) production and DNA damage were still detected [6]. Similar effects have also been observed on trapped bacterial cells where, for example, it was shown that a 1064 nm laser could inhibit the growth and division of *E. coli* cells at laser power as low as 3 mW [7,8], and dose ranging from 0.54 J to over 10 J[9]. In addition, it was shown that bacterial cells trapped in optical tweezers are less efficient at regulating their pH, indicating disruption of the membrane [10].

As mentioned above, how laser light interacts and the effects on a trapped bacterial cell have previously been investigated. However, a gap exists in the literature regarding the effects of laser light on bacterial spores. While optical tweezers and LTRS in combination are widely used to manipulate spores and measure various properties, such as classification of sporulated and germinated forms, response to heat treatment, changes in chemical composition and surface properties [11,1,12–16], any effect of the incident laser light on the spore has not been considered thoroughly. Spores are resilient, dehydrated inactive forms that some bacteria species can convert to when under stress. Spores are strongly resistant to, for example, chemical and thermal damage [17], where spores have several mechanisms to protect their DNA [18]. Thus, a higher resistance to any photoinduced (photothermal and/or photochemical) damage by the laser light is expected compared to vegetative bacterial cells or eukaryotic cells.

In this work we address the photoinduced damage from a laser beam on spores and how it might affect the experimental results by monitoring the intensity of the CaDPA main Raman peak using a LTRS instrument. CaDPA is found in abundance in the spore core (protecting the DNA), making up to 25 % of its dry weight, and has a strong characteristic Raman peak at 1017 cm^{-1} [1,19]. Therefore, when the intensity of this peak is reduced, we know that CaDPA is lost from the spore core, most likely by spore body disruption and diffusion to surrounding medium. This approach also allows us to investigate how different decontamination protocols affect the CaDPA loss [9], allowing many common spore decontamination agents such as hydrogen peroxide, sodium hypochlorite, and peracetic acid [20] to be investigated. Sodium hypochlorite and peracetic acid are oxidizing agents used as decontamination chemicals where sodium hypochlorite acts by saponification of fatty acids and neutralization and chloramination of amino acids, [21] and peracetic acid oxidazes, for example, sulfhydryl and sulfur bonds [22].

Finally, to gain further insight in the mechanisms of the interaction between the laser light and the spore, we also support the experimental data and conclusions with a multiphysics simulation model of a spore to estimate any photothermal contribution.

2. Experimental methods

2.1. LTRS system

To measure Raman spectra from spores, we use our optical trap and Laser Tweezers Raman instrument that is described in [23,24]. Briefly, a Gaussian laser beam operating at 808 nm is coupled into the microscope using a dichroic shortpass mirror with a cut off wavelength of 650 nm. Imaging and focusing of the beam is done by a 60× water immersion objective (UPlanSApo, Olympus) with a numerical aperture of 1.2 and a working distance of 0.28 mm. This provides a diffraction limited spot diameter in the focal plane of ~nm.

We measure Raman spectra by collecting the back-scattered light with the microscope objective and the Rayleigh scattrered light is reduced by a notch filter (NF808-34, Thorlabs) [24]. To increase the signal to noise ratio, we spatially filter the beam using a 150 μm diameter pinhole before coupling the light into our spectrometer (Model 207, McPherson) through a 150 μm wide entrance slit and an 800 grooves/mm holographic grating disperses the light onto a Peltier cooled 2D CCD detector (Newton 920 N-BR-DD XW-RECR, Andor) operated at −95 °C. Our setup has a spectral resolution of <2 cm^{-1} in Raman shift.

2.2. Sample preparation and measurements

A stock of *Bacillus thuringiensis* (*B. thuringiensis*) ATCC 35646 spore suspension is made with a concentration of 10^6 spores per ml. To re-suspend the spore stock, we vortex them at 2,800 rpm (VM3 Vortex, M. Zipperer GmBH) for 10 s. A sample is made by adding a 1 cm diameter ring of 1 mm thick vacuum grease on a 24 mm × 60 mm glass coverslip. Then we add 5 μl of the spore suspension inside the ring and seal the sample by placing a 23 mm × 23 mm cover slip on top. We then place the sample in the LTRS-system and locate a single free floating spore for Raman measurements. The system has an inherent selectivity as only objects with sufficient symmetric shape and refractive index contrast remain in the trap, thus allowing Raman spectra collection. Raman spectra presented herein are recorded by using 2 accumulations. The acquisition time depends on the laser power used, from 30 s for 5 mW laser power to 5 s for 40 mW laser power and spectra were captured until the main CaDPA peak vanished or during a maximum of 90 min.

2.3. SEM imaging

To perform SEM imaging, we air dry a drop of spore suspension on a glass slide. We then coat the sample with a ~5 nm layer of platinum using a Quorum Q150T-ES sputter coater. We image samples by a Carl Zeiss Merlin FESEM electron microscope using InLens and SE-2 imaging modes at a magnification of 50,000×.

2.4. TEM imaging

We prepare samples for TEM imaging as a liquid suspension of spores using the method described in [16]. Spores are fixed with 2.5% Glutaraldehyde in 0.1 M PHEM buffer and postfixed in 1% aqueous osmium tetroxide, then dehydrated in ethanol, acetone, and finally embedded in Spurr's resin. 70 nm sections are then post contrasted in uranyl acetate and Reynold's lead citrate. We examine samples using a Talos L120C (FEI, Eindhoven, The Netherlands) operating at 120 kV. Micrographs were acquired with a Ceta 16 M CCD camera.

2.5. Spectrophotometry measurements

We measure the absorbance of liquid solutions using a Lambda 1050+ UV/VIS/NIR spectrophotometer (PerkinElmer). To remove scattered light signal from that of the absorbed light, we use an accompanied integrating sphere with a center mount cuvette (UV grade quartz, l = 10 mm, Mettler Toledo) sample holder. We dissolve our materials in suitable solvents as listed below. We pour 3 ml of the solution into cuvettes and measure the absorbance in the wavelength range of 700–1200 nm. This absorbance is then compared to that of the lone solvent to extract the absorbance of the spore material. 30 mM DPA and 1% d-DNA (Sigma-Aldrich) solutions in deionised water were analyzed as representative of the core and 1% Soy Phospholipid in ethanol (Sigma Aldrich) as representative of the membrane. To extract the solubilized spore coat from *B. thuringiensis* spores, we used sodium deocyl sulphate + dithiothreitol and the sodium hydroxide methods described in [25,26]. We confirmed the loss of spore coat by TEM microscopy.

2.6. Numerical modeling

To simulate the interaction between the spore and the laser light, we build a numerical 3D-model of a spore in water using COMSOL Multiphysics 5.5 software. The spore is constructed as a six-layer ellipsoid, with dimensions 1000 nm × 700 nm, similar to the model described in [27]. The layers represent, from inside out, the core (700 nm × 400 nm), membrane (23 nm thick), cortex (85 nm), coat (40 nm), interspace (111 nm), and exosporium (40 nm) of the spore. See schematic as inset in Fig. 1.

Each layer is given a set of parameters. Spore parameters such as real part of the refractive index [28,29] and thermal conductivity [30–33] were gathered from literature. To find the complex part of the refractive index, k, we measure absorbance of the spore components (spore coat, CaDPA, DNA and phospholipid). From the absorbance we convert values for the complex refractive index of the spore layers: core ($k = 6 \times 10^{-7}$), membrane ($k = 5.5 \times 10^{-7}$), cortex ($k = 4.5 \times 10^{-7}$), coat ($k = 2 \times 10^{-6}$), interspace ($k = 2 \times 10^{-7}$), and exosporium ($k = 2 \times 10^{-6}$).

We use a high resolution mesh inside and close to the spore, while keeping the rest coarse. The mesh size in the volume closest to the spore is 10 nm and growing to 500 nm at a distance 10 μm from the center of the spore.

We model the laser beam to represent the experimental setup using the Wave Optics Module. To model the heating effect on the spore we use the Heat Transfer and the Wave Optics Module in combination. We then use this model to simulate the temperature increase in a spore placed in the laser beam focus of our LTRS system.

To validate the model, we place a cube with known dimensions and thermal parameters in the focus of the simulated laser beam. By comparing the temperature change obtained from the simulation to that of the theoretically calculated average temperature of the cube, we determine that the model accurately simulates that system within 30%.

2.7. Statistical method

Considering the nature of data, where the peak intensity remains constant over different times after which a rapid decay until vanishing occurs, survival plot analysis was performed on some of the data sets in Graphpad Prism 9. Different data sets were also compared using the Mantel-Cox test.

3. Results and discussion

3.1. Laser power effect on spores in water

For samples with weak Raman peaks or when the LTRS instrument has inefficient collecting optics, higher laser power is often applied to shorten the integration time. To monitor the influence of laser power on spores, the time to signal loss of the CaDPA Raman peak was investigated for laser powers of 5, 20 and 40 mW in the sample plane. (Note that the highest value, 40 mW, in this study is still lower than some works reported in the literature.)

As mentioned earlier, CaDPA has a strong characteristic Raman peak at 1017 cm^{-1} (see Fig. 1) and the rapid decay of this peak is a good indicator of spore core leakage due to damage [34]. Thus, we monitored the intensity of the 1017 cm^{-1} peak and the time to complete decay for a number of individual spores. We present these data sets as Survival plots as shown in Fig. 2. See also Fig. S1 for an example behavior of the CaDPA peak over time. We believe the spore decomposition is triggered by the high intensity of light passing through the spore and generating reactive species that degrade the spore. We have also created a model of a spore in a focused 40 mW laser to determine if thermal or electric field can contribute to the spore decomposition observed (see Sections 3.4 and 3.5).

For a laser power of 5 mW, which is more-or-less the lower limit used in LTRS for spores in the literature [11,1,12–14,19], all investigated spores remain intact over the duration of the experiments (90 min), however, 20 and 40 mW laser power clearly has an effect on analyzed spores, see Fig. 2.

We observed that the lifetime of the spores (defined as time from start of exposure until 1017 cm^{-1} Raman peak vanishes) when trapped at 40 mW ranges from 1.5 to 50 min (3.6–120 J total energy exposure), with one outlier at 72 min (173 J). The median survival time is 24 min (58 J) (n = 25). By comparison, when trapping spores at 20 mW laser power, the lifetime ranged from 4.5 to over 90 min (5.4–108 J total energy), with a median survival time of 48.5 min (58 J) (n = 25), with four spores (16%) retaining the CaDPA peak until we stopped the measurement, as shown in Fig. 2. The difference between the survival times at 40 mW and 20 mW is significant (p = 0.0008). As mentioned, when further decreasing the power to the lower limit, 5 mW, spores (n = 10) do not lose their CaDPA over the measurement time (27 J). The 5 mW result is consistent with previous studies, indicating no CaDPA release when using low laser power in LTRS setups [35,16]. Compared to reported values for vegetative bacterial cells [9], spores require a significantly higher dose for noticeable damage. It it also notable that the total energy for spores to lose DPA (58 J median) is approximately 2 orders of magnitude greater than the energies reported to inactivate *E. coli* bacteria (0.54 J) [9] highlights the resilience of spores to damage.

Parallel to a rapid release of CaDPA, as monitored by the loss of 1017 cm^{-1} peak intensity, the spores also lose their contrast when viewed in the optical microscope and tend to fall out from the optical trap, suggesting a large alteration of the spore body. To better assess and visualize this alteration, we deposited eight laser damaged spores on a cover-slip using the LTRS system and imaged them using SEM. The SEM images reveal that all spores that lost the CaDPA Raman signal during the LTRS measurement appear collapsed, see Fig. 1D, compared to unexposed spores which appear to retain their structure intact see Fig. 1C. Since the spores appear significantly damaged in the SEM, after optical trapping at high laser powers, they were most likely not viable after losing the CaDPA (which embeds and protects the DNA).

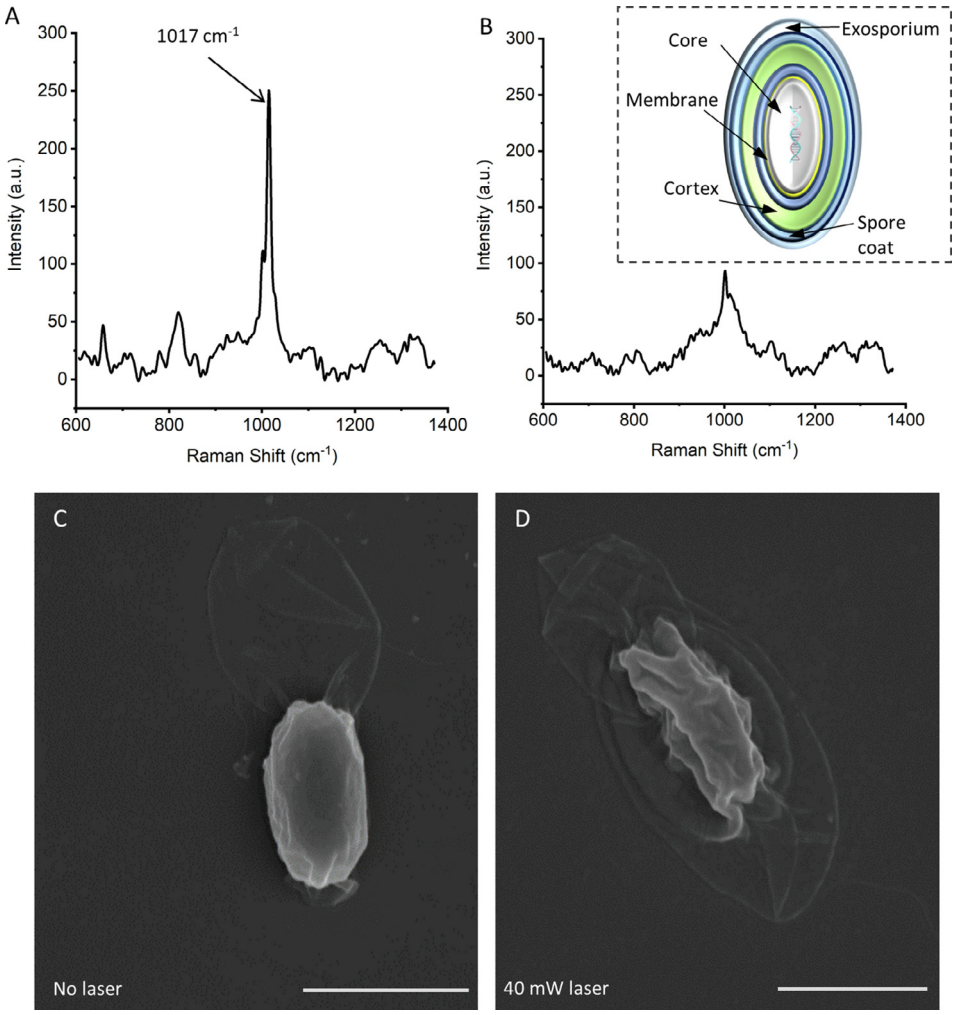

Fig. 1. Spore Raman spectra and SEM micrographs (representative images for a sample size of n = 50 untreated spores and n = 10 laser-trapped spores). A) An LTRS spectrum of a spore before losing the CaDPA peak at 1017 cm^{-1} and B) after the CaDPA Raman peak vanished. C) Shows SEM micrograph of an unexposed spore, and D) shows a SEM micrograph of a spore that lost the CaDPA Raman peak during a LTRS measurements at 40 mW. Scale bars are 1 μm. Inset in B): A schematic representation of a bacterial spore and its multi-layer structure.

3.2. Laser power affects spore CaDPA lifetime in peracetic acid

Peracetic acid is an effective sporicidal chemical known to deactivate spores by several log within 1 min [36,20], and with our own data showing a 5 log reduction in 1 min [16] for the concentration used herein. We investigated the effect of laser power on the CaDPA Raman peak lifetime similar as described in the subsection above. Again, the laser power affected the lifetime, where already a laser power of 5 mW induced a CaDPA loss (interpreted as a damage of the spore coat) and shorter lifetimes was observed for spores trapped with a 20 mW laser ($p < 0.0001$), see Fig. 3. The median survival time was 9.2 min for 20 mW power (11 J), compared to 22.7 min at 5 mW (27 J). There was also a significant difference between spores deactivated by peracetic acid compared to spores in water ($p < 0.0001$), i.e., this chemical deactivation make the spores more susceptible to laser induced damage. Note, however, that spores unexposed to laser light appear intact over the whole duration of the experiments (90 min) and that time in peracetic acid did not affect the lifetimes, see Figs. S3 and S5C-D. Peracetic acid deactivate spores by oxidation of bonds such as sulfhydryl and sulfur bonds [22], in the case of spores by targeting the spore membrane [37,38]. This weakening of the membrane may then reduce the overall resistance for, e.g., ROS resulting in spore body damage and subsequent loss of CaDPA already at low (5 mW) laser power.

3.3. Degradation rate of spores in sodium hypochlorite increase in a laser beam

Sodium hypochlorite is another sporicidal chemical that also can significantly alter the body of the spore as seen in TEM images, see Fig. S5A-B. In a previous work, on a smaller sample size, we noted similarities in the DPA release for peracetic acid and sodium hypochlorite [16], and also recorded a 1 log reduction in viable spores after 1 min and a 5 log reduction after 10 min, that is, a slower rate of deactivation as compared to peracetic acid for concentrations used in this study. We also observed that the spores degrade completely after longer exposure time to sodium hypochlorite and that no spores could be found and trapped after 50 min of immersion (Fig. S4, S5B), that is, there exists a chemically induced component on similar time scale as the possible laser induced effects.

To assess the laser light influence on CaDPA loss from spores in hypochlorite, we exposed spores to a 0.5% solution and measured the lifetime of the CaDPA Raman peak, see Fig. 4. In this case, however, the measurements revealed an additional dependence on the

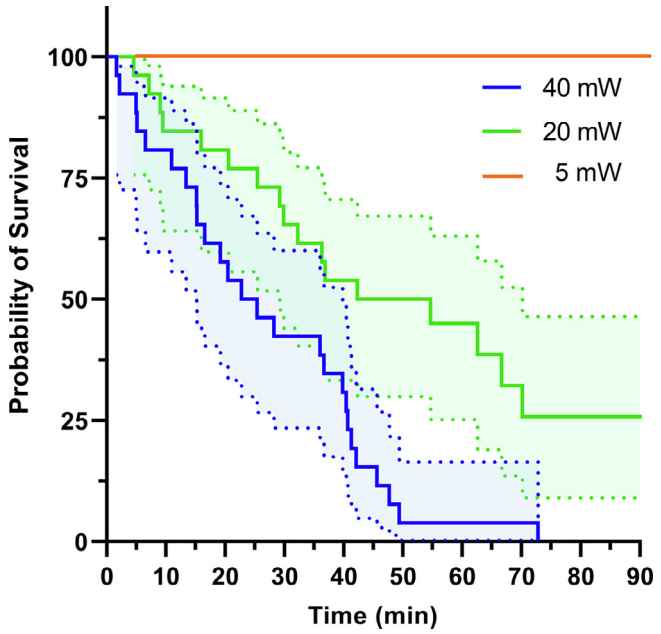

Fig. 2. Survival analysis plots for spores in deionised water trapped in the LTRS at 5 (n = 10), 20 (n = 25) and 40 mW (n = 25), respectively. The 50% survival corresponds to the median time to CaDPA loss for the spores. The solid lines are the actual survival times, and the shaded region represents a 95% confidence interval. Note that each "death" event represents a loss of the spore's CaDPA peak with an associated lifetime.

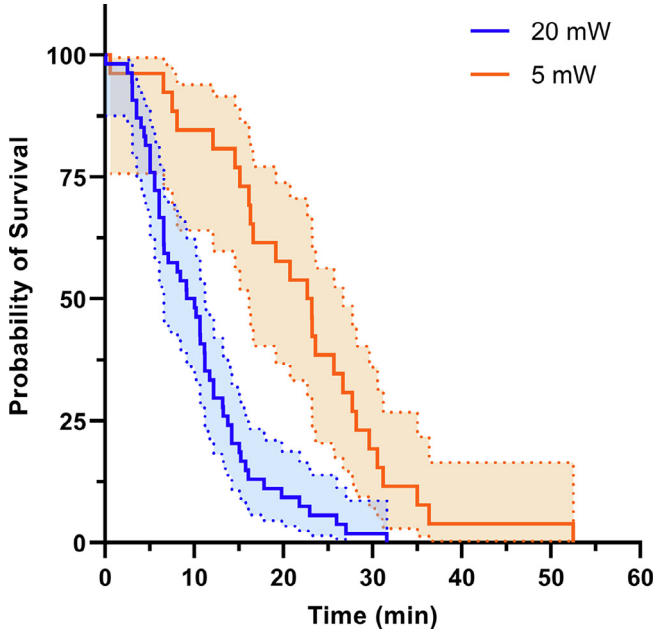

Fig. 3. Survival analysis plots for spores deactivated in 1% peracetic acid, trapped in LTRS and analyzed at 5 mW and 20 mW (n = 25 for each plot). Again, each "death" event represents a loss of the spore's CaDPA peak with an associated lifetime.

total time in sodium hypochlorite, which could not be observed for spores in water and peracetic acid, see Figs. S2 and S3. This effect is not entirely unexpected and can be explained by the mechanism of action of hypochlorite and its degradation effects on spores over time.

To better illustrate the data, we plot the lifetime of the characteristic CaDPA peak when trapped in LTRS against the pre-incubation time in sodium hypochlorite. There is a clear dependence on time in hypochlorite solution and CaDPA lifetime, where the mean lifetime decreases for longer exposure to the decontamination chemical. In addition, a higher laser power further decreases the lifetime of the CaDPA peak, see Fig. 4.

For 5 mW power, our data indicate that even this low power can affect the spore. If the laser beam did not influence the spores, we would expect to have at least some trapped spores with CaDPA lifetime comparable to 50 min. However, 99% of spores with a pre-incubation time between 0 and 10 min time were degraded in the LTRS measurement within a total time of 25 min, which is significantly shorter than the expected degradation time. This is consistent at longer pre-incubation times: at 10–20 min pre-incubation time, 99% of spores were degraded in the LTRS measurement within a total time of 35 min. That 5 mW laser power should have an effect on spores is further supported by TEM images. Spores appear visually intact (Fig. S5A) after 5 min exposure to sodium hypochlorite, after which a continuous chemical degradation takes place as indicated by the TEM micrograph at 30 min (Fig. S5B).

For laser powers of 10 and 20 mW it is clear that the degradation is further enhanced by the laser light, see Fig. 4, as the average lifetimes are reduced in comparison to 5 mW. The mean lifetimes for spore CaDPA loss within the 0–10 min interval, were 7.8 min at 5 mW (2.3 J), 5.6 min at 10 mW (3.4 J) and 3.2 min at 20 mW (3.9 J). Note that for 20 mW laser power, average lifetimes for all intervals are similar, further confirming the effect from the laser light.

3.4. Numerical modeling indicates negligible laser heating

To gain further insight in the mechanisms involved in the laser beam induced spore degradation and subsequent release of chemicals at higher laser powers, we created a 3D multiphysics simulation model to estimate the laser induced heating. We modeled a spore in water exposed to a focused Gaussian laser beam (TEM_{00} mode). In this model we included all spore layers, i.e., from the innermost layer to the outermost; the core, membrane, cortex, coat, interspace, and exosporium. Relevant values for the layers are given in the method section.

The spore was modelled in the focus of a 40 mW, 808 nm Gaussian laser beam, see Fig. 5A. Laser light penetrates the spore, which refracts and absorbs light based on the refractive indices of the spore layers. Because of the relatively low absorbance of the different spore building blocks at 808 nm, we expect only a slight increase of the temperature of the spore, also supported by previous studies found in the literature [39,40].

Considering thermal effects from the laser, we found the overall spore temperature to increase by <200 mK while exposed to the beam. The temperature increased from 293.15 K to 293.32 K, see Fig. 5C. This increase is within the expected values at similar wavelengths [39,40]. To confirm the robustness of the simulation, we increase the complex refractive index values in all the spore layers by a factor of 100. This resulted in an overall 100-fold temperature increase, thus yielding a spore temperature of 303 K, further indicating the physicality of our model. Smaller increases on the order 10% to the complex refractive index increased the overall spore temperature by 0.02 K, suggesting small changes in complex refractive index do not significantly alter the results of our model. Within and between spore layers, we did not see any significant temperature differences. Temperature changes of the order 100 mK can be considered negligible and unlikely to cause thermal damage to the spore, indicating that the damage induced by the laser on the spore is non-thermal.

3.5. Numerical modeling shows high localised electric fields, inducing electron polarisation

We found the electric field surrounding the spore to be around 3 MV/m, see Fig. 5B from the simulation. A high electric field is

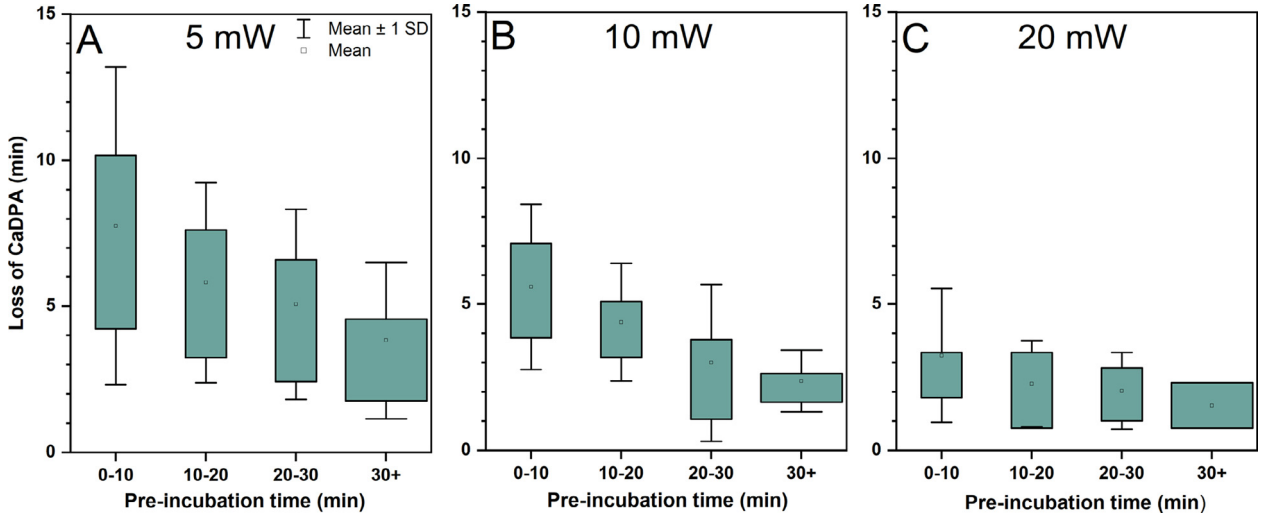

Fig. 4. Time for CaDPA release from spores in sodium hypochlorite during LTRS compared to the pre- incubation time clustered in 10 min intervals for three laser powers. A) 5 mW (n = 142) B) 10 mW (n = 75) C) 20 mW (n = 112). A one minute resolution plot of all data is shown in Fig. S4.

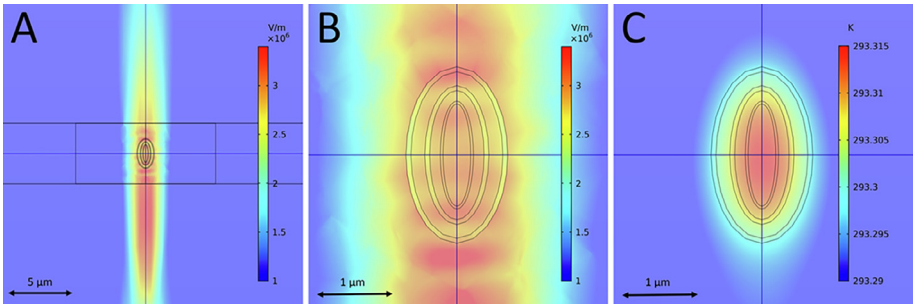

Fig. 5. A 3D model of a spore in the focus of a 808 nm Gaussian laser beam (A). Differences in absorption by spore layers are seen. The focus of the laser beam generates an electric field on the order of 3 MV/m surrounding the spore (B). The spore absorbs parts of the EM-radiation, resulting in a temperature increase in the order of 100 mK (C).

expected, owing to the highly focused laser beam with a waist of approximately 400 nm. At the frequency of near infrared electromagnetic radiation ($\sim 10^{14}$ Hz), the primary interaction of the field with the sample is by electron polarisation of the sample. Unlike, for example, microwave interaction, which can change the orientation of polar molecules, electron polarisation is lossless why there is no sample heating from this interaction [41]. However, electron polarisation can contribute to reactions, including that of enzymes as detailed in literature [42–44]. Considering the high electric field, such a polarisation-enhanced reaction speed could be a contributing factor to the effects observed at higher laser powers. In future work, modeling the polarisation similar to as described in [45] could be beneficial.

There were small but not insignificant (approximately 25%) differences in the electric field between layers, with the protein coat and exosporium experiencing a weaker electric field than surrounding layers because of their higher refractive indicies. Additionally, the difference in refractive indices between layers induce a bending of the electric field. This bending results in a pattern of alternating high and low electric field strengths along the beam path. The parts of the spore exposed to more intense laser irradiance, as indicated by a stronger electric field, may then be subject to an increased probability of photochemical reactions such as the generation of ROS resulting in a more rapid degradation of the spore.

4. Conclusion

Optical tweezers combined with micro-Raman spectroscopy are valuable tools for investigating bacterial spores. However, any effect of the trapping laser on the spore must be noted. Spores are normally considered very resilient to environmental stress, but as we show in this work they can be affected when trapped in a NIR laser beam. We show that for high laser powers 40 mW, which has been used in some studies, the laser beam can affect and disrupt the spore directly in pure water. We show with our experimental data and our multiphysics model that this spore disruption is laser power dependent but likely not of photothermal character. We also show that even at low laser powers, down to 5 mW, the laser may have an effect on spores deactivated by different chemicals, such as spore deactivation by peracetic acid or sodium hypochlorite. We hope this study highlights the effects of optical tweezers on spores and that this effect may need to be taken into account.

CRediT authorship contribution statement

Dmitry Malyshev: Conceptualization, Methodology, Investigation, Formal Analysis, Writing – original draft, Writing – review & editing. **Rasmus Öberg:** Methodology, Investigation, Formal Analysis, Writing – review & editing. **Tobias Dahlberg:** Software, Resources. **Krister Wiklund:** Methodology, Formal Analysis. **Lars Landström:** Resources, Writing – review & editing. **Per Ola Andersson:** Resources, Writing – review & editing. **Magnus Andersson:** Conceptualization, Methodology, Supervision, Project administration, Funding acquisition, Resources, Writing – original draft, Writing – review & editing.

Declaration of Competing Interest

The authors declare that they have no known competing financial interests or personal relationships that could have appeared to influence the work reported in this paper.

Acknowledgements

This work was supported by the Swedish Research Council (2019-04016); the Umeå University Industrial Doctoral School (IDS); Kempestiftelserna (JCK-1916.2); and Swedish Department of Defence, Project No. 470-A400821. We thank Anna-Lena Johansson at FOI for providing the original stock of spores for this project.

The authors acknowledge the facilities and technical assistance of the Umeå Core Facility for Electron Microscopy (UCEM) at the Chemical Biological Centre (KBC), Umeå University, a part of the National Microscopy Infrastructure NMI (VR-RFI 2016-00968)

Appendix A. Supplementary material

Supplementary data associated with this article can be found, in the online version, at https://doi.org/10.1016/j.saa.2021.120381.

References

[1] S.-S. Huang, D. Chen, P.L. Pelczar, V.R. Vepachedu, P. Setlow, Y.-Q. Li, Levels of Ca2+-Dipicolinic Acid in Individual Bacillus Spores Determined Using Microfluidic Raman Tweezers, J. Bacteriol. 189 (2007) 4681–4687, https://doi.org/10.1128/JB.00282-07.

[2] K. Svoboda, S.M. Block, Optical trapping of metallic Rayleigh particles, Opt. Lett. 19 (1994) 930–932, https://doi.org/10.1364/OL.19.000930.

[3] K.J. Aufderheide, Q. Du, E.S. Fry, Directed Positioning of Micronuclei in Paramecium tetraurelia with Laser Tweezers: Absence of Detectible Damage After Manipulation, J. Eukaryot. Microbiol. 40 (1993) 793–796, https://doi.org/10.1111/j.1550-7408.1993.tb04476.x.

[4] H. Schneckenburger, A. Hendinger, R. Sailer, M.H. Gschwend, W.S.L. Strauss, M. Bauer, K. Schutze, Cell viability in optical tweezers: high power red laser diode versus Nd:YAG laser, J. Biomed. Opt. 5 (2000) 40, https://doi.org/10.1117/1.429966.

[5] S.K. Mohanty, A. Rapp, S. Monajembashi, P.K. Gupta, K.O. Greulich, Comet assay measurements of DNA damage in cells by laser microbeams and trapping beams with wavelengths spanning a range of 308 nm to 1064 nm, Radiat. Res. 157 (2002) 378–385, https://doi.org/10.1667/0033-7587(2002)157[0378:CAMODD]2.0.CO;2.

[6] S.K. Mohanty, M. Sharma, P.K. Gupta, Generation of ROS in cells on exposure to CW and pulsed near-infrared laser tweezers, Photochem. Photobiol. Sci. 5 (2006) 134–139, https://doi.org/10.1039/B506061C.

[7] S. Ayano, Y. Wakamoto, S. Yamashita, K. Yasuda, Quantitative measurement of damage caused by 1064-nm wavelength optical trapping of Escherichia coli cells using on-chip single cell cultivation system, Biochem. Biophys. Res. Commun. 350 (2006) 678–684, https://doi.org/10.1016/j.bbrc.2006.09.115.

[8] U. Mirsaidov, W. Timp, K. Timp, M. Mir, P. Matsudaira, G. Timp, Optimal optical trap for bacterial viability, Phys. Rev. E 78 (2008) 021910, https://doi.org/10.1103/PhysRevE.78.021910.

[9] Y. Zhang, Z. Miao, X. Huang, X. Wang, J. Liu, G. Wang, Laser Tweezers Raman Spectroscopy (LTRS) to Detect Effects of Chlorine Dioxide on Individual Nosema bombycis Spores, Appl. Spectrosc. 73 (2019) 774–780, https://doi.org/10.1177/0003702818817522.

[10] M.B. Rasmussen, L.B. Oddershede, H. Siegumfeldt, Optical Tweezers Cause Physiological Damage to Escherichia coli and Listeria Bacteria, Appl. Environ. Microbiol. 74 (2008) 2441–2446, https://doi.org/10.1128/AEM.02265-07.

[11] J.W. Chan, A.P. Esposito, C.E. Talley, C.W. Hollars, S.M. Lane, T. Huser, Reagentless Identification of Single Bacterial Spores in Aqueous Solution by Confocal Laser Tweezers Raman Spectroscopy, Anal. Chem. 76 (2004) 599–603, https://doi.org/10.1021/ac0350155.

[12] P. Zhang, P. Setlow, Y. Li, Characterization of single heat-activated Bacillus spores using laser tweezers Raman spectroscopy, Opt. Express 17 (2009) 16480, https://doi.org/10.1364/OE.17.016480.

[13] L. Kong, P. Setlow, Y.-Q. Li, Observation of the dynamic germination of single bacterial spores using rapid Raman imaging, J. Biomed. Opt. 19 (2013) 011003, https://doi.org/10.1117/1.jbo.19.1.011003.

[14] G. Pesce, G. Rusciano, A. Sasso, R. Isticato, T. Sirec, E. Ricca, Surface charge and hydrodynamic coefficient measurements of Bacillus subtilis spore by optical tweezers, Colloids surf. B Biointerfaces 116 (2014) 568–575, https://doi.org/10.1016/j.colsurfb.2014.01.039.

[15] S. Wang, J. Yu, M. Suvira, P. Setlow, Y.-Q. Li, Uptake of and Resistance to the Antibiotic Berberine by Individual Dormant, Germinating and Outgrowing Bacillus Spores as Monitored by Laser Tweezers Raman Spectroscopy, PLOS ONE 10 (2015) e0144183, https://doi.org/10.1371/journal.pone.0144183.

[16] D. Malyshev, T. Dahlberg, K. Wiklund, P.O. Andersson, S. Henriksson, M. Andersson, Mode of Action of Disinfection Chemicals on the Bacterial Spore Structure and Their Raman Spectra, Anal. Chem. 93 (2021) 3146–3153, https://doi.org/10.1021/acs.analchem.0c04519.

[17] G.C. Stewart, The Exosporium Layer of Bacterial Spores: a Connection to the Environment and the Infected Host, Microbiol. Mol. Biol. Rev. 79 (2015) 437–457, https://doi.org/10.1128/MMBR.00050-15.

[18] P. Setlow, Spore Resistance Properties, Microbiology Spectrum 2 (2014) 1–14, https://doi.org/10.1128/microbiolspec.TBS-0003-2012.

[19] S. Wang, P. Setlow, Y.-Q. Li, Slow Leakage of Ca-Dipicolinic Acid from Individual Bacillus Spores during Initiation of Spore Germination, J. Bacteriol. 197 (2015) 1095–1103, https://doi.org/10.1128/JB.02490-14.

[20] M.J. Leggett, J. Spencer Schwarz, P.A. Burke, G. McDonnell, S.P. Denyer, J.Y. Maillard, Mechanism of sporicidal activity for the synergistic combination of peracetic acid and hydrogen peroxide, Appl. Environ. Microbiol. 82 (2016) 1035–1039, https://doi.org/10.1128/AEM.03010-15.

[21] C. Estrela, C.R. Estrela, E.L. Barbin, J.C.E. Spanó, M.A. Marchesan, J.D. Pécora, Mechanism of action of sodium hypochlorite, Braz. Dental J. 13 (2002) 113–117, https://doi.org/10.1590/S0103-64402002000200007.

[22] G. McDonnell, A.D. Russell, Antiseptics and disinfectants: activity, action, and resistance, Clin. Microbiol. Rev. 12 (1999) 147–179, https://doi.org/10.1128/CMR.12.1.147, URL: http://www.ncbi.nlm.nih.gov/pubmed/9880479.

[23] T. Stangner, T. Dahlberg, P. Svenmarker, J. Zakrisson, K. Wiklund, L.B. Oddershede, M. Andersson, Cooke-Triplet tweezers: more compact, robust, and efficient optical tweezers, Opt. Lett. 43 (2018) 1990, https://doi.org/10.1364/ol.43.001990.

[24] T. Dahlberg, D. Malyshev, P.O. Andersson, M. Andersson, Biophysical fingerprinting of single bacterial spores using laser Raman optical tweezers, Chemical, Biological, Radiological, Nuclear, and Explosives (CBRNE) Sensing XXI, SPIE (2020) 28, https://doi.org/10.1117/12.2558102.

[25] W. Donovan, L. Zheng, K. Sandman, R. Losick, Genes encoding spore coat polypeptides from Bacillus subtilis, J. Mol. Biol. 196 (1987) 1–10, https://doi.org/10.1016/0022-2836(87)90506-7.

[26] N.C. Thorne, H.N. Shah, S.E. Gharbia, Isolation and Preparation of Spore Proteins and Subsequent Characterisation by Electrophoresis and Mass Spectrometry, in: Mass Spectrometry for Microbial Proteomics, 3, John Wiley and Sons Ltd, Chichester, UK, 2010, pp. 143–156.

[27] D. Malyshev, C.F. Williams, J. Lees, L. Baillie, A. Porch, Model of microwave effects on bacterial spores, J. Appl. Phys. 125 (2019), https://doi.org/10.1063/1.5085442.

[28] K.M. Siegrist, E. Thrush, M. Airola, A.K. Carr, D.M. Limsui, N.T. Boggs, M.E. Thomas, C.C. Carter, Water absorption in a refractive index model for bacterial spores, Chemical, Biological, Radiological, Nuclear, and Explosives (CBRNE) Sensing X 7304 (2009) 73040C, https://doi.org/10.1117/12.818863.

[29] A. Katz, A. Alimova, M. Xu, P. Gottlieb, E. Rudolph, J.C. Steiner, R.R. Alfano, In situ determination of refractive index and size of Bacillus spores by light transmission, Opt. Lett. 30 (2005) 589, https://doi.org/10.1364/OL.30.000589.

[30] R.G. Leuschner, P.J. Lillford, Thermal properties of bacterial spores and biopolymers, Int. J. Food Microbiol. 80 (2003) 131–143, https://doi.org/10.1016/S0168-1605(02)00139-3.

[31] B.M. Foley, C.S. Gorham, J.C. Duda, R. Cheaito, C.J. Szwejkowski, C. Constantin, B. Kaehr, P.E. Hopkins, Protein Thermal Conductivity Measured in the Solid State Reveals Anharmonic Interactions of Vibrations in a Fractal Structure, J. Phys. Chem. Lett. 5 (2014) 1077–1082, https://doi.org/10.1021/jz500174x.

[32] . Xue, S. Lofland, X. Hu, Thermal Conductivity of Protein-Based Materials: A Review, Polymers 11 (2019) 456, https://doi.org/10.3390/polym11030456.

[33] A.R.N. Bastos, C.D.S. Brites, P.A. Rojas-Gutierrez, C. DeWolf, R.A.S. Ferreira, J.A. Capobianco, L.D. Carlos, Thermal Properties of Lipid Bilayers Determined Using Upconversion Nanothermometry, Adv. Funct. Mater. 29 (2019) 1905474, https://doi.org/10.1002/adfm.201905474.

[34] L. Kong, P. Setlow, Y.-Q. Li, Analysis of the Raman spectra of Ca2+-dipicolinic acid alone and in the bacterial spore core in both aqueous and dehydrated environments, Analyst 137 (2012) 3683, https://doi.org/10.1039/c2an35468c.

[35] D. Chen, S.S. Huang, Y.Q. Li, Real-time detection of kinetic germination and heterogeneity of single Bacillus spores by laser tweezers Raman spectroscopy, Anal. Chem. 78 (2006) 6936–6941, https://doi.org/10.1021/ac061090e.

[36] W.A. Rutala, D.J. Weber, Guideline for disinfection and sterilization in healthcare facilities, Centers Dis. Control Prevent. (2008) www.cdc.gov/infectioncontrol/guidelines/disinfection/index.html.

[37] B. Setlow, G. Korza, K. Blatt, J. Fey, P. Setlow, Mechanism of Bacillus subtilis spore inactivation by and resistance to supercritical CO 2 plus peracetic acid, J. Appl. Microbiol. 120 (2016) 57–69, https://doi.org/10.1111/jam.12995.

[38] M.J. Leggett, J.S. Schwarz, P.A. Burke, G. Mcdonnell, S.P. Denyer, J.-Y. Maillard, Resistance to and killing by the sporicidal microbicide peracetic acid, J. Antimicrob. Chemother. 70 (2015) 773–779, https://doi.org/10.1093/jac/dku445.

[39] B. del Rosal, P. Haro-González, W.T. Ramsay, L.M. Maestro, K. Santacruz-Gómez, M.C. Iglesias-de la Cruz, F. Sanz-Rodríguez, J.Y. Chooi, P. Rodríguez-Sevilla, D. Choudhury, A.K. Kar, J. García Solé, L. Paterson, D. Jaque, Heat in optical tweezers, Opt. Trap. Opt. Micromanipul. X 8810 (2013) 88102A, https://doi.org/10.1117/12.2027750.

[40] F. Català, F. Marsà, M. Montes-Usategui, A. Farré, E. Martín-Badosa, Influence of experimental parameters on the laser heating of an optical trap, Sci. Rep. 7 (2017) 16052, https://doi.org/10.1038/s41598-017-15904-6.

[41] F. Bibi, M. Villain, C. Guillaume, B. Sorli, N. Gontard, A review: Origins of the dielectric properties of proteins and potential development as bio-sensors, Sensors (Switzerland) 16 (2016) 1–21, https://doi.org/10.3390/s16081232.
[42] Y. Xiang, L. Duan, J.Z.H. Zhang, Protein's electronic polarization contributes significantly to its catalytic function, J. Chem. Phys. 134 (2011) 205101, https://doi.org/10.1063/1.3592987.
[43] X. Wang, Y. Li, X. He, S. Chen, J.Z.H. Zhang, Effect of Strong Electric Field on the Conformational Integrity of Insulin, J. Phys. Chem. A 118 (2014) 8942–8952, https://doi.org/10.1021/jp501051r.
[44] L.L. Duan, G.Q. Feng, Q.G. Zhang, Large-scale molecular dynamics simulation: Effect of polarization on thrombin-ligand binding energy, Sci. Rep. 6 (2016) 31488, https://doi.org/10.1038/srep31488.
[45] O.M. Szklarczyk, S.J. Bachmann, W.F. van Gunsteren, A polarizable empirical force field for molecular dynamics simulation of liquid hydrocarbons, J. Comput. Chem. 35 (2014) 789–801, https://doi.org/10.1002/jcc.23551.